

# Energetics-based Protein Profiling on a Proteomic Scale: Identification of Proteins Resistant to Proteolysis

Chiwook Park, Sharleen Zhou, Jacqueline Gilmore and Susan Marqusee\*

Department of Molecular and Cell Biology and QB3 Institute, University of California, Berkeley, Berkeley CA 94720-3206, USA

Native states of proteins are flexible, populating more than just the unique native conformation. The energetics and dynamics resulting from this conformational ensemble are inherently linked to protein function and regulation. Proteolytic susceptibility is one feature determined by this conformational energy landscape. As an attempt to investigate energetics of proteins on a proteomic scale, we challenged the *Escherichia coli* proteome with extensive proteolysis and determined which proteins, if any, have optimized their energy landscape for resistance to proteolysis. To our surprise, multiple soluble proteins survived the challenge. Maltose binding protein, a survivor from thermolysin digestion, was characterized by *in vitro* biophysical studies to identify the physical origin of proteolytic resistance. This experimental characterization shows that kinetic stability is responsible for the unusual resistance in maltose binding protein. The biochemical functions of the identified survivors suggest that many of these proteins may have evolved extreme proteolytic resistance because of their critical roles under stressed conditions. Our results suggest that under functional selection proteins can evolve extreme proteolysis resistance by modulating their conformational energy landscapes without the need to invent new folds, and that proteins can be profiled on a proteomic scale according to their energetic properties by using proteolysis as a structural probe.

© 2007 Elsevier Ltd. All rights reserved.

**Keywords:** protein folding; energy landscape; proteolysis; proteomics; proteolytic susceptibility

\*Corresponding author

## Introduction

Proteins do not adopt unique, static structures; they access many different conformations within the native state ensemble.<sup>1–3</sup> This ensemble includes small fluctuations around the native conformation, partially unfolded forms, and even the globally unfolded form. The population of each conformation is determined by its stability according to a Boltzmann distribution. These populations, combined with the dynamics of interconversion among conformations, define the conformational energy land-

scape of a protein. This energy landscape is encoded within the amino acid sequence, and underlies biological properties such as catalysis, signal transduction, and protein turnover.<sup>4–7</sup> Thus, the entire energy landscape is subject to the same types of evolutionary pressures as is the native structure.

In spite of the great interest in energy landscapes, experimental determinations of energetic information on protein conformations have been slow, requiring purification of individual proteins and investigation with traditional biophysical instrumentation. These limitations have impeded acquiring a system-wide perspective on protein energetics. What is the distribution of kinetic and thermodynamic stabilities of proteins within a proteome? Is there a biological reason for the difference in conformational energy landscapes between proteins? Are the conformational energy landscapes of orthologous proteins conserved along with their structures and functions? These questions demand a new approach to studying protein energetics.

Present address: C. Park, Department of Medicinal Chemistry and Molecular Pharmacology, Purdue University, West Lafayette, IN 47907-2091, USA.

Abbreviations used: MBP, maltose binding protein; PDB, Protein Data Bank.

E-mail address of the corresponding author: [marqusee@uclink.berkeley.edu](mailto:marqusee@uclink.berkeley.edu)

Here we report an investigation of proteolytic susceptibility as an attempt for energetic profiling of proteins on a proteomic scale. A protein's susceptibility to proteolytic digestion is a functional attribute linked to its energy landscape.<sup>8–10</sup> In order to be cleaved, the substrate polypeptide chain must be extended to fit into the substrate-binding sites of a protease,<sup>11</sup> which make compactly folded proteins poor substrates for proteolysis. Proteolysis of compactly folded proteins requires access to high-energy cleavable states, where cleavage sites are exposed to proteases through local or global unfolding (Figure 1(a)).<sup>8,12–14</sup> Proteolytic susceptibility of folded proteins, therefore, is determined by the thermodynamic or kinetic accessibility of these cleavable states. The nominal energy landscape diagrams in Figure 1(b) depict how proteolytic susceptibility is dictated by energy landscapes. Each diagram shows the energy levels of folded, intermediate, and globally unfolded states. When a protein has an unstructured region in its native conformations, the protein can be cleaved by a protease without unfolding (1 in Figure 1(b)). Proteins 2 and 3 show different global stability but the same susceptibility, while proteins 3 and 4 have the same global stability but different susceptibility. Protein 5 has a cleavable

state relatively low in energy but a high kinetic barrier to access the cleavable state, which confers the protein's proteolytic resistance. A protein's proteolytic susceptibility is, therefore, determined by its conformational energy landscape and not by its global stability.<sup>8,15</sup>

Recent studies on the protein  $\alpha$ -lytic protease provide an unusual example of a conformational energy landscape resistant to proteolysis.<sup>16</sup> This protein, itself a protease in a harsh extracellular environment, ensures proteolytic resistance with an unusually high kinetic barrier to unfolding (local or global). How unusual are proteins whose energy landscapes encode resistance to proteolysis? We need to determine proteolytic susceptibility of proteins on a proteomic scale to answer this question. To profile proteins according to their proteolytic susceptibility in a high-throughput fashion, we devised a survival assay, where proteins in a cell lysate are subjected to extensive proteolysis; the survivors are then identified using genomic data. We chose the proteome of *Escherichia coli* for our first investigation.

## Results

### Extensive proteolysis of an *E. coli* lysate

Proteolytic digestion was carried out on an *E. coli* K12 lysate prepared from an overnight culture. In the first assay, the lysate was digested with 0.40 mg/ml trypsin (approximately 5–10% of the total protein in the reaction) at 25 °C for four days, and the reaction was monitored by SDS-PAGE (Figure 2(a)). A significant number of proteins were digested within the first 30 min; some proteins, however, survived proteolysis and were visible throughout the four-day experiment.

Trypsin cleaves specifically after lysine and arginine residues, and some proteins with proteolytically sensitive conformations may survive the assay due to this specificity. We therefore repeated the same survival assay using thermolysin (0.40 mg/ml at 25 °C), which cleaves before hydrophobic and aromatic residues (Ile, Leu, Val, Ala, Met, Phe).<sup>17</sup> Again, many proteins survived this four-day incubation (Figure 2(b)). Even more survivors were observed with thermolysin than with trypsin. The differences are not surprising, since the proteases have different catalytic activities and specificities. The results, however, clearly indicate that there are also survivors to a protease with broader substrate specificity than trypsin.

In order to account for any loss in protease activity due to autodigestion during the course of the assay, protease activity was monitored over the four-day incubation. No apparent decrease in protease activity was observed under our reaction conditions where 10 mM CaCl<sub>2</sub> was included (data not shown), suggesting that survival is indeed a consequence of a protein's resistance to proteolysis within the experimental time scale.

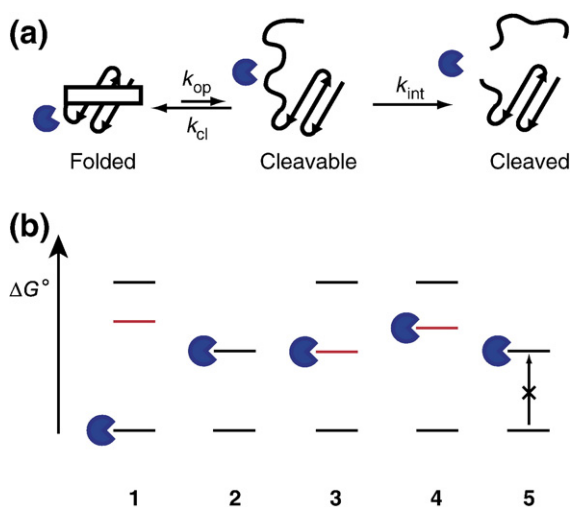


**Figure 1.** Proteolysis of proteins under native conditions. (a) Schematic representation of the mechanism of proteolytic cleavage of a protein in its native state. Proteins without flexible loops or unstructured regions in the folded conformation are protected from proteolysis. These proteins are cleaved only by accessing cleavable states.  $k_{op}$ ,  $k_{cl}$ , and  $k_{int}$  are the kinetic constants for opening, closing, and intrinsic proteolysis steps, respectively. (b) Nominal energy landscape of proteins to explain proteolytic susceptibility. Lowest lines in the energy diagram indicate native forms, and the highest lines indicate fully unfolded forms. Lines in red indicate the cleavable states between folded and globally unfolded states. Proteins with flexible loops or unstructured regions (1) are digested even in their native conformation. Otherwise, proteins need to unfold fully (2), or transform to a cleavable form (3 and 4), to be digested. Kinetic barriers can also result in resistance to proteolysis by making it difficult to access the cleavable state, which is low in energy (5).

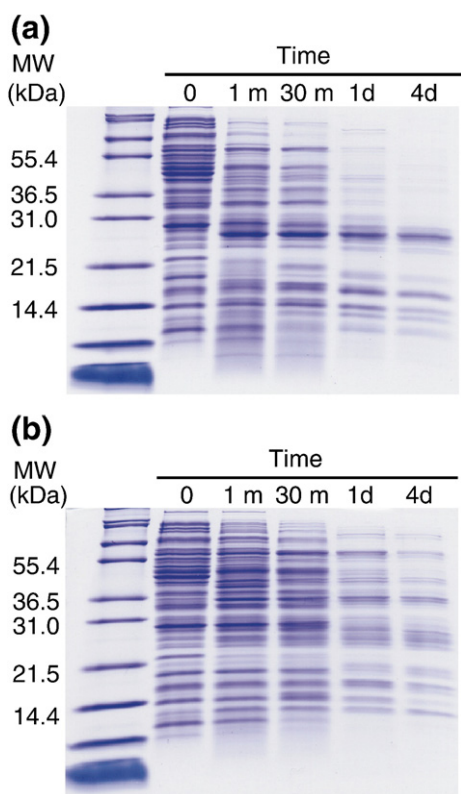


**Figure 2.** Digestion of *E. coli* lysate with trypsin. (a) SDS-PAGE gel of samples taken at the designated time points from the proteolysis reaction of *E. coli* lysate by 0.40 mg/ml trypsin. (b) SDS-PAGE gel of samples taken at the designated time points from the proteolysis reaction of *E. coli* lysate by 0.40 mg/ml thermolysin.

### Identification of survivors

We used two-dimensional (2-D) gel electrophoresis to identify survivors. An *E. coli* K12 lysate was incubated with 0.40 mg/ml trypsin or thermolysin. The reactions were quenched after one day and four days. Comparison of 2-D gels of one-day digestion and four-day digestion allowed us to monitor any apparent decrease in intensity between one day and four days. We selected 30 spots from 2-D gels of four-day trypsin digestion and 40 spots from 2-D gels of four-day thermolysin digestion (Figure 3 and Table 1). To minimize the redundancy of the identified proteins, only one spot was chosen when a series of spots exist in a horizontal arrangement, which frequently indicate variants of one protein with different charges due to modifications during sample preparation. Spots showing any noticeable decrease in intensity from one-day to four-day digestion are indicated in Table 1. Proteins corresponding to these spots are likely to have the minimal resistance required to survive the current challenge. The same amount of untreated lysate was also run on a 2-D gel to estimate roughly how many proteins in *E. coli* proteome are sampled with the current approach. About 500

spots were observed from the cell lysate with the staining method used in this study.

Selected spots were analyzed using peptide-mass mapping by matrix-assisted laser desorption ionization- time of flight (MALDI-TOF) to identify proteins (Table 1). A protein is considered as a survivor only when the molecular mass of the protein estimated from the gel matches within 10% with that expected from the sequence. Using this approach, we identified 22 survivors from digestion with trypsin and 34 survivors from digestion with thermolysin (Table 2). Sixteen of the identified trypsin survivors (73%) were also identified as thermolysin survivors (Figure 4 and Table 2). The existence of so many common survivors suggests that the survival is not due to substrate specificities of the proteases but due to the unusual energy landscapes of the survivors. The apparent *pI* values of most survivors are consistent with the calculated *pI* values. Any inconsistent *pI* values

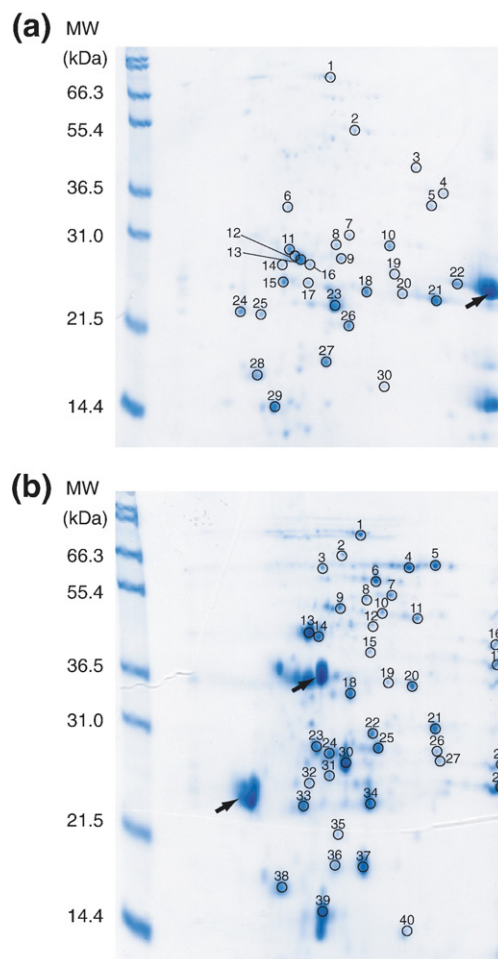


**Figure 3.** Identification of survivors by 2-D electrophoresis. *E. coli* soluble fraction digested with 0.40 mg/ml trypsin (a) or 0.40 mg/ml thermolysin (b) for four days were analyzed by 2-D electrophoresis. The numbers on the gels indicate the spots analyzed by in-gel digestion and mass spectrometry. The identity of the protein in each spot is listed in Table 1. Black arrows indicate spots corresponding to proteases.

**Table 1.** Identification of proteins from 2-Dimensional electrophoresis gels

Spot number	Protein ID	Gene name	Length	$M_r$ (kDa)	$pI$
<i>A. Identified proteins from spots on the 2-D gel of E. coli lysate digested with 0.40 mg/ml trypsin for four days</i>					
1	P21179	<i>katE</i>	753	84.2	5.54
2	P06715	<i>Gor</i>	450	48.8	5.64
3	P76108	<i>ydcS</i>	359	40.0	6.27
4	P06977	<i>gapA</i>	330	35.4	6.58
5	P25887	<i>yghA</i>	294	31.4	6.32
6	P60651	<i>speB</i>	306	33.6	5.14
7	P24223	<i>pdxJ</i>	242	26.3	5.61
8 <sup>a</sup>	P00882	<i>deoC</i>	259	27.7	5.50
9	P04790	<i>tpiA</i>	255	27.0	5.64
10	P02925	<i>rbsB</i>	271	28.5	5.99
11	P09551	<i>argT</i>	238	25.8	5.22
12	P12758	<i>udp</i>	252	27.0	5.81
13	P12758	<i>udp</i>	252	27.0	5.81
14	P75743	<i>ybgI</i>	247	26.9	5.07
15	P21367	<i>ycaC</i>	208	23.1	5.20
	P32661	<i>rpe</i>	225	24.6	5.13
16	P12758	<i>udp</i>	252	27.0	5.81
17 <sup>a</sup>	P12758	<i>udp</i>	252	27.0	5.81
18	P09743	<i>deoD</i>	238	25.8	5.42
19	P10344	<i>ghnH</i>	226	25.0	6.87
20	P00448	<i>sodA</i>	205	23.0	6.44
21	P00448	<i>sodA</i>	205	23.0	6.44
22	P10344	<i>ghnH</i>	226	25.0	6.87
23	P09157	<i>sodB</i>	192	21.1	5.58
24	P09157	<i>sodB</i>	192	21.1	5.58
25 <sup>a</sup>	P17288	<i>ppa</i>	175	19.6	5.03
26 <sup>b</sup>	P04790	<i>tpiA</i>	255	27.0	5.64
27 <sup>b</sup>	P12758	<i>udp</i>	252	27.0	5.81
28 <sup>a</sup>	P11056	<i>bfr</i>	158	18.5	4.69
29 <sup>b</sup>	P27430	<i>dps</i>	166	18.6	5.72
30	P23827	<i>eco</i>	142	16.1	5.94
<i>B. Identified proteins from spots on the 2-D gel of E. coli lysate digested with 0.40 mg/ml thermolysin for four days</i>					
1	P21179	<i>katE</i>	753	84.2	5.54
2 <sup>a</sup>	P07024	<i>ushA</i>	525	58.2	5.40
3 <sup>a</sup>	P13482	<i>treA</i>	535	60.5	5.36
4	P14178	<i>pykF</i>	470	50.7	5.77
5 <sup>a</sup>	P23843	<i>oppA</i>	517	58.4	5.85
6	P00391	<i>ipdA</i>	473	50.6	5.79
7	P06715	<i>gor</i>	450	48.8	5.64
8 <sup>a</sup>	P22259	<i>pckA</i>	540	59.6	5.46
9 <sup>a</sup>	P19926	<i>agp</i>	391	43.6	5.38
10	P37095	<i>pepB</i>	427	46.2	5.60
11 <sup>a</sup>	P75691	<i>yahK</i>	349	38.0	5.80
12	P00509	<i>aspC</i>	396	43.6	5.54
13	P11665	<i>Pgk</i>	386	41.0	5.08
14	P02928	<i>malE</i>	370	40.7	5.22
15	P31133	<i>potF</i>	344	38.3	5.53
16	P76108	<i>ydcS</i>	359	40.0	6.27
17 <sup>a</sup>	P06977	<i>gapA</i>	330	35.4	6.58
18	P13652	<i>cdd</i>	294	31.5	5.42
19 <sup>b</sup>	P14178	<i>pykF</i>	470	50.7	5.77
20 <sup>b</sup>	P14178	<i>pykF</i>	470	50.7	5.77
21	P02925	<i>rbsB</i>	271	28.5	5.99
22	P00882	<i>deoC</i>	259	27.7	5.50
23	P09551	<i>argT</i>	238	25.8	5.22
24	P30859	<i>artI</i>	224	25.0	5.32
25	P04790	<i>tpiA</i>	255	27.0	5.64
26	P32697	<i>aphA</i>	212	23.5	5.94
27	P10344	<i>ghnH</i>	226	25.0	6.87
	P30860	<i>artJ</i>	224	24.9	5.97
28	P10344	<i>ghnH</i>	226	25.0	6.87
29	P00448	<i>sodA</i>	205	23.0	6.44
30	P12758	<i>udp</i>	252	27.0	5.81
31	P21367	<i>ycaC</i>	208	23.1	5.20
32	P32661	<i>rpe</i>	225	24.6	5.13
33	P17288	<i>ppa</i>	175	19.6	5.03

**Table 1 (continued)**

Spot number	Protein ID	Gene name	Length	$M_r$ (kDa)	$pI$
<i>B. Identified proteins from spots on the 2-D gel of E. coli lysate digested with 0.40 mg/ml thermolysin for four days</i>					
34	P09157	<i>sodB</i>	192	21.1	5.58
35 <sup>b</sup>	P07651	<i>deoB</i>	407	44.4	5.11
36 <sup>a,b</sup>	P12758	<i>Udp</i>	252	27.0	5.81
37 <sup>b</sup>	P12758	<i>Udp</i>	252	27.0	5.81
38	P11056	<i>Bfr</i>	158	18.5	4.69
39	P27430	<i>Dps</i>	166	18.6	5.72
40 <sup>b</sup>	P05313	<i>aceA</i>	434	47.5	5.16

<sup>a</sup> The spot intensity has been decreased noticeably compared with the same spot on the 2-D gel of the lysate digested for one day under the same condition.

<sup>b</sup> The size of the peptide estimated from the gel suggests that the spot corresponds to a fragment from proteolysis of the protein.

may indicate posttranslational modifications or oxidation during the incubation.

### Sequence analysis of survivors

To identify any general rules that encode survival to such extensive proteolysis, we looked for common features within the amino acid compositions of the survivors. An analysis of amino acid composition shows that the survivors from trypsin digestion contain plenty of lysine and arginine residues, potential trypsin cleavage sites. Lysine/arginine residues comprise 10.4(±2.6)% of the total number of residues of each survivor. For comparison, we determined the average lysine/arginine content of all open reading frames in the *E. coli* genome to be 10.3(±3.4)%. Resistance to digestion is not due to a lack of potential cleavage sites.

$\alpha$ -Lytic protease, a bacterial enzyme known for its kinetic stability and protease resistance, has 16% glycine residues, while its proteolysis-sensitive homolog chymotrypsin has only 9% glycine residues. This high glycine content was proposed to be a structural factor that enables tight and cooperative packing within the core of this protein.<sup>18</sup> We determined the average glycine content of all identified survivors to be 7.6(±1.6)%, which is clearly much lower than that for  $\alpha$ -lytic protease and more in line with our determination for the average glycine content of all open reading frames in the *E. coli* genome, 7.1(±2.5)%. Therefore, the high glycine content is not likely to be a common reason for proteolytic resistance.

### Proteolysis kinetics of maltose binding protein

To confirm the validity of the proteomic survival assay, we cloned, expressed, and purified maltose binding protein (MBP), a survivor identified from thermolysin digestion, but not from trypsin digestion. Digestion of purified MBP by 0.40 mg/ml thermolysin was so slow that the reaction was monitored for 20 days. The kinetic constant for the proteolysis of MBP by 0.40 mg/ml thermolysin was

**Table 2.** Identified survivors

Gene name	Description	PDB ID	Subunits	Localization
<i>Common survivors</i>				
<i>katE</i>	Catalase HPII	1GGE	4	
<i>gor</i>	Glutathione reductase	1GET	2	
<i>ycdS</i>	Putative periplasmic binding protein, ydcS			Periplasmic <sup>b</sup>
<i>gapA</i>	Glyceraldehyde-3-phosphate dehydrogenase A	1GAD	4	
<i>deoC</i>	Deoxyriboaldolase	1JCL	2	
<i>tpiA</i>	Triosephosphate isomerase	1TRE	2	
<i>rbsB</i>	Ribose binding periplasmic protein	2DRI	1	Periplasmic
<i>argT</i>	LAO-binding periplasmic protein		1	Periplasmic
<i>udp</i>	Uridine phosphorylase	1K3F	6	
<i>ycaC</i>	ycaC	1YAC	8	
<i>rpe</i>	Ribulose phosphate 3-epimerase			
<i>glnH</i>	Glutamine-binding periplasmic protein	1WDN	1	Periplasmic
<i>sodA</i>	Superoxide dismutase (Mn)	1D5N	2	
<i>sodB</i>	Superoxide dismutase (Fe)	1ISA	2	
<i>ppa</i>	Inorganic phosphatase	1JFD	6	
<i>bfr</i>	Bacterioferritin	1BFR	24	
<i>Identified as survivors only in trypsin digestion</i>				
<i>yghA</i>	Hypothetical oxidoreductase, yghA			
<i>speB</i>	Agmatinase			
<i>pdxJ</i>	PNP synthase	1M5W	8	
<i>ybgI</i>	Hypothetical UPF0135 protein ybgI	1NMO	6 <sup>a</sup>	
<i>deoD</i>	Purine nucleoside phosphorylase	1A69	6	
<i>eco</i>	Ecotin	1ECY	2	Periplasmic
<i>Identified as survivors only in thermolysin digestion</i>				
<i>ushA</i>	UDP-sugar hydrolase (5'-nucleotidase)	1HP1	1	Periplasmic
<i>treA</i>	Trehalase		1	Periplasmic
<i>pykF</i>	Pyruvate kinase I	1PKY	4	
<i>oppA</i>	Periplasmic oligopeptide-binding protein		1	Periplasmic
<i>ipdA</i>	Dihydrolipoyl dehydrogenase		2	
<i>pckA</i>	Phosphoenolpyruvate carboxykinase	1AYL	1	
<i>agp</i>	Glucose-1-phosphatase	1NT4	2	Periplasmic
<i>pepB</i>	Peptidase B		6	
<i>yahK</i>	yahK (alcohol dehydrogenase-like)	1UUF	2 <sup>a</sup>	
<i>aspC</i>	Aspartate aminotransferase	1AAW	2	
<i>pgk</i>	Phosphoglycerate kinase		1	
<i>malE</i>	Maltose binding protein	1ANF	1	Periplasmic
<i>potF</i>	Putrescine-binding protein	1A99	1	Periplasmic
<i>cdd</i>	Cytidine deaminase	1CTT	2	
<i>artI</i>	Arginine-binding protein 1		1	Periplasmic <sup>b</sup>
<i>aphA</i>	Class B acid phosphatase	1N8N	4	Periplasmic <sup>b</sup>
<i>artJ</i>	Arginine-binding protein 2		1	Periplasmic <sup>b</sup>
<i>dps</i>	DNA protection during starvation protein	1DPS	12	

Information on each protein was collected from Swiss-Prot/TrEMBL (<http://www.us.expasy.org/sprot/>). Only periplasmic proteins are indicated so in the localization column.

<sup>a</sup> The quaternary structure of this protein is based on the structure determined by X-ray crystallography and is not confirmed under physiological conditions.

<sup>b</sup> The localization information on this protein is inferred from sequence analyses and is not determined experimentally.

determined to be  $1.2 \times 10^{-6} \text{ s}^{-1}$ , corresponding to a half life of 6.6 days, which confirmed the result of the survival assay on a proteomic scale. MBP was also digested with 0.40 mg/ml trypsin with a greater rate constant,  $4.4 \times 10^{-5} \text{ s}^{-1}$  (half life = 4.3 h), which is also consistent with the result that MBP was not found as a survivor from the tryptic digestion of *E. coli* lysate. Unfolded MBP was observed to be quite susceptible to thermolysin,<sup>19</sup> indicating that the structure of this protein protects it from being digested by proteases.

To understand the physical origin of MBP's resistance to proteolysis by thermolysin, we determined proteolysis kinetics of the protein at different thermolysin and trypsin concentration (Figure 5). When proteolysis of a protein occurs by the kinetic

mechanism shown in Figure 1(a), the overall proteolysis rate constant ( $k_p$ ) is expressed as:

$$k_p = \frac{k_{op} \cdot k_{int}}{k_{cl} + k_{int}}, \quad (1)$$

where  $k_{op}$  and  $k_{cl}$  are the rate constants for the forward and the backward reaction from the folded state to the cleavable state, and  $k_{int}$  is the intrinsic proteolysis rate for an unstructured peptide. When  $k_{int}$  is estimated as the product of  $k_{cat}/K_m$  and protease concentration ( $[E]$ ),<sup>8</sup> equation (1) can be rewritten as:

$$k_p = \frac{k_{op}[E]}{\frac{k_{op}}{K_{op}(k_{cat}/K_M)} + [E]}, \quad (2)$$

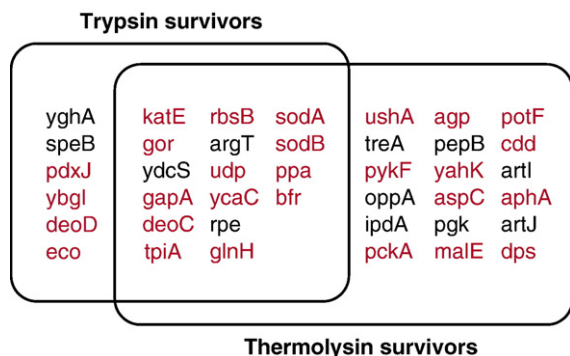


**Figure 4.** Common survivors from assays with trypsin and thermolysin. The proteins in the overlapping region survived four-day digestion with 0.40 mg/ml trypsin and 0.40 mg/ml thermolysin. For convenience, gene names are used for corresponding proteins. The proteins shown in red have structural coordinates deposited in the protein data bank [<http://www.rcsb.org/pdb/>].

where  $K_{op}$  ( $=k_{op}/k_{cl}$ ) is the equilibrium constant between the folded and the cleavable states in Figure 1(a).<sup>8</sup> By determining  $k_p$  at different concentrations of a protease, we can determine  $k_{op}$  and  $K_{op}$  of the opening step leading to the cleavable conformation. When  $k_{cl} \gg k_{int}$ , however, equation (1) is simplified as:

$$k_p = K_{op}k_{int} = K_{op}(k_{cat}/K_M)[E], \quad (3)$$

by which we can only determine  $K_{op}$ .

The plot of the proteolysis rates of MBP determined at different thermolysin concentrations shows an asymptotic behavior (Figure 5(a)), suggesting that the kinetics to access the cleavable state in MBP ( $k_{op}$  in Figure 1(a)) determines the overall proteolysis rate at high concentration of protease. However, the rate of proteolysis of MBP by trypsin is linearly dependent on the protease concentration without any indication of the asymptotic pattern shown in proteolysis by thermolysin (Figure 5(b)), indicating that  $k_{cl} \gg k_{int}$  under the given assay condition. By fitting  $k_p$  of proteolysis by thermolysin to equation (2),  $k_{op}$  and  $K_{op}$  were determined to be  $1.8 \times 10^{-6} \text{ s}^{-1}$  and  $4.9 \times 10^{-7}$ . The  $k_p$  values of proteolysis by trypsin were fit to equation (3), and  $K_{op}$  was determined to be  $8.3 \times 10^{-6}$ . To determine  $K_{op}$ ,  $k_{cat}/K_M$  values measured with peptide substrates were used: ABZ-Ala-Gly-Leu-Ala-pNA for thermolysin ( $7.3 \times 10^5 \text{ M}^{-1}\text{s}^{-1}$ ) and insulin  $\beta$ -chain for trypsin ( $3.0 \times 10^5 \text{ M}^{-1}\text{s}^{-1}$ ).<sup>19,20</sup>

The  $k_{op}$  value for proteolysis by thermolysin ( $1.8 \times 10^{-6} \text{ s}^{-1}$ ) is in a quite good agreement with the global unfolding rate constant for MBP determined by urea denaturation ( $1.3 \times 10^{-6} \text{ s}^{-1}$ ). This result strongly suggests that proteolysis of MBP by thermolysin is limited by the same kinetic barrier limiting global unfolding. The energies of the cleavable states for thermolysin and trypsin digestion are calculated to be 8.6 kcal/mol and 6.9 kcal/mol, respectively, with the determined  $K_{op}$  values. We also determined the global stability of

MBP ( $\Delta G_{unf}^\circ$ ) to be  $14.6(\pm 0.7) \text{ kcal/mol}$  by monitoring unfolding of the protein in urea by circular dichroism. The smaller energies of the cleavable states than  $\Delta G_{unf}^\circ$  suggest that the proteolysis of MBP occurs through intermediate states, not through a globally unfolded state.

## Discussion

### Structures of survivors

Seventeen out of the 22 trypsin survivors (77%) and 24 out of 34 thermolysin survivors (71%) have had their structures solved by X-ray crystallography (Figure 4 and Table 2). This unusually high proportion of proteins with known structures suggests that proteolytically resistant proteins are advantageous for X-ray crystallography, perhaps due to ease of crystallization or purification. Inspection of these available protein structures did not reveal any common structural features to explain their proteolytic resistance. The gallery of structures in Figure 6 does not reveal any characteristic structural ele-

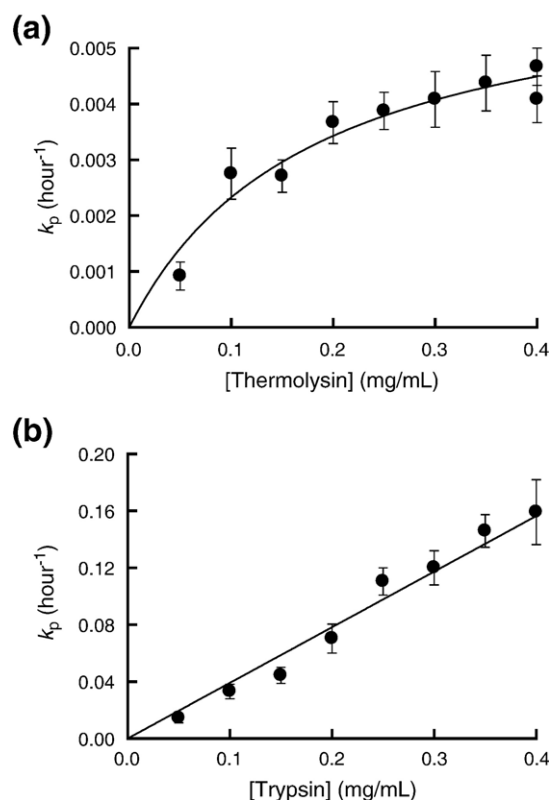


**Figure 5.** Proteolysis mechanism of MBP by thermolysin and trypsin. MBP was incubated at 25 °C with 0.40 mg/ml thermolysin (a) or 0.40 mg/ml trypsin (b) in 20 mM Tris-HCl buffer (pH 8.0) containing 50 mM NaCl and 10 mM CaCl<sub>2</sub>. The  $k_p$  values for thermolysin digestion were fit to equation (2) to determine  $k_{op}$  and  $K_{op}(k_{cat}/K_M)$ . From the  $k_p$  values for trypsin digestion only  $K_{op}(k_{cat}/K_M)$  value was determined by a linear regression using equation (3).

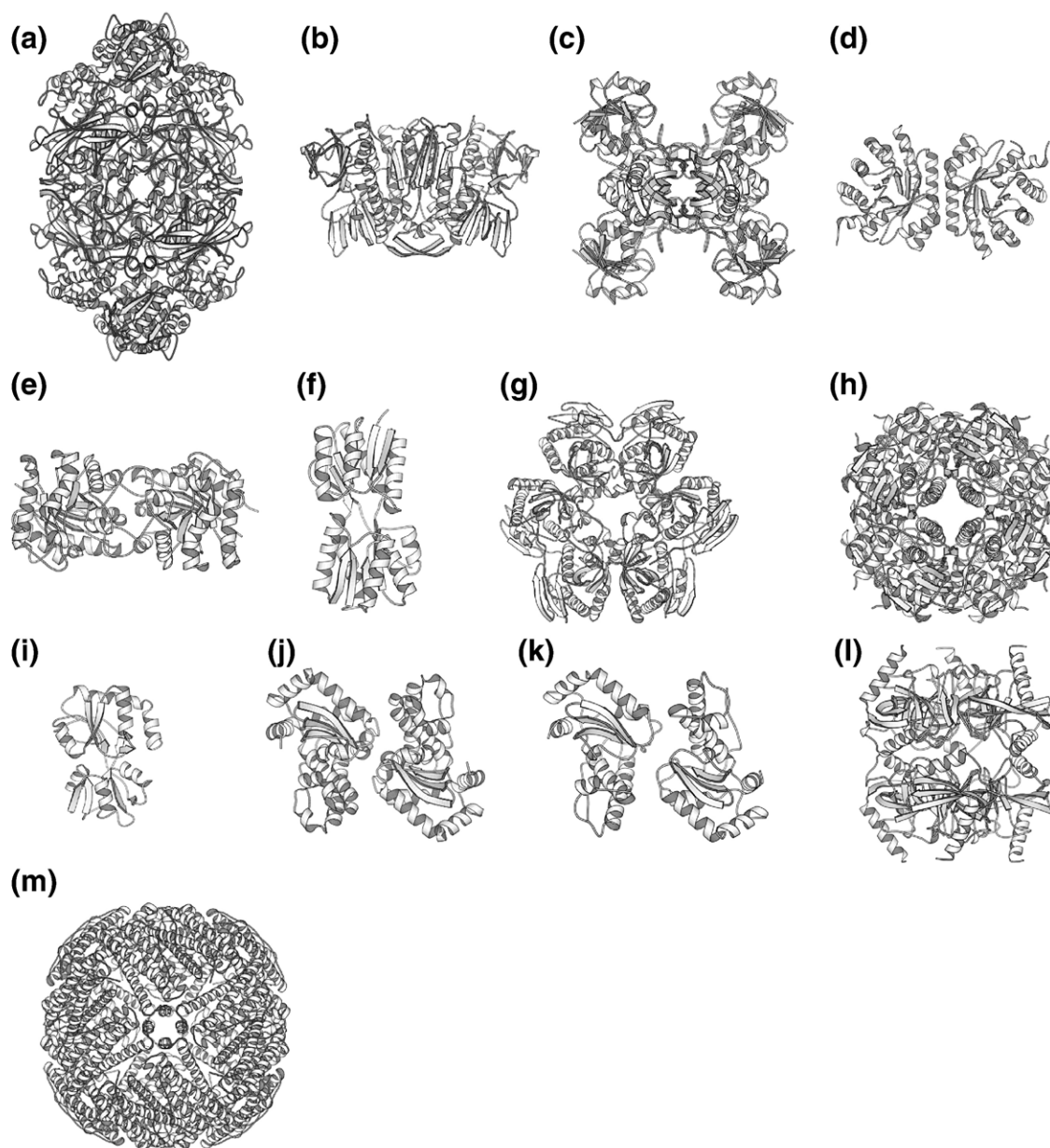


**Figure 6.** Ribbon representation of the structures of proteins that survived both trypsin and thermolysin. Structures of assumed biological molecules are shown for multimeric proteins. (a) Catalase HPII (PDB entry: 1GGE). (b) Glutathione reductase (PDB entry: 1GET). (c) Glyceraldehyde-3-phosphate dehydrogenase A (PDB entry: 1GAD). (d) Deoxyriboaldolase (PDB entry: 1JCL). (e) triosephosphate isomerase (PDB entry: 1TRE). (f) Ribose binding periplasmic protein (PDB entry: 2DRI). (g) Uridine phosphorylase (PDB entry: 1K3F). (h) *ycaC* (1YAC). (i) Glutamine-binding periplasmic protein (PDB entry: 1WDN). (j) Manganese superoxide dismutase (PDB entry: 1D5N). (k) Iron superoxide dismutase (PDB entry: 1ISA). (l) Inorganic pyrophosphatase (PDB entry: 1JFD). (m) Bacterioferritin (PDB entry: 1BFR). Ribbon diagrams were made with the program MOLSCRIPT.<sup>41</sup>

ments, such as tight loops, specific arrangement of secondary structures, or common motifs. For instance, only four out of 28 proteins with known structures have disulfide bonds: ecotin, UDP-sugar hydrolase, glucose-1-phosphatase, and putrescine-binding protein. Therefore, there does not seem to be any specific structure or fold required for protease resistance, again suggesting a fine-tuning of the energy landscape.

The wide array of protein folds observed among the survivors (Figure 6) is perhaps not surprising.

Thermophilic proteins encode significantly different thermodynamic properties from their mesophilic homologs, even though they have the same three-dimensional folds.<sup>21,22</sup> Apparently, just like the thermophilic proteins, under functional selection the survivors have evolved such extreme protease resistance by modulating their conformational energy landscapes without the need to invent new structures or folds.

Proteolytic resistance does not apparently imply a lack of conformational change or allostery. For

instance, the periplasmic binding proteins switch from open forms to closed forms when they bind to their cognate ligands.<sup>23,24</sup> Inorganic pyrophosphatase, purine nucleotide phosphorylase, and glyceraldehyde-3-phosphate dehydrogenase are multimeric enzymes that show cooperativity in their catalysis.<sup>25–27</sup> Survival of these proteins suggests that these dynamic processes do not necessarily result in proteolytically susceptible conformations.

The survivors comprise a group of diverse quaternary structures (Table 2). Because the energetics of oligomeric proteins is dependent on protein concentration, proteolytic susceptibility of these proteins could be dependent on protein concentration. Since the protein concentration in the survival assay is much lower than their concentrations *in vivo*, survivors in this dilute condition would be still resistant at protein concentrations close to those *in vivo*. Several of the survivors are also known to bind various cofactors including metals. The observed resistance may reflect a property of holoenzymes complexed with cofactors. It should be noted, however, that the free cofactor concentrations in the assay must be quite low because the lysate used in this study was carefully dialyzed.

### Resistance to proteolysis and biological functions

Energy landscapes encoding such apparent rigidity may be an important functional feature subject to natural selection. Many of the survivors in Table 2 belong to two categories of biochemical functions: a family of periplasmic binding proteins and a group of stress-related proteins. It is important to note that our screen was not comprehensive and is undoubtedly biased by the culture conditions and experimental protocol. Absence of a protein from the list should not imply proteolysis sensitivity.

Nine of the identified survivors are periplasmic binding proteins (Table 2). This appears particularly significant, considering *E. coli* has only ~40 periplasmic binding proteins.<sup>28</sup> Periplasmic proteins of *E. coli* are likely to be more exposed to exogenous proteases than are cytosolic proteins. The presence of ecotin, one of the survivors and an endogenous protease inhibitor in *E. coli* periplasm, indicates the necessity of protection against exogenous proteases in the periplasmic space. Our results suggest that proteolytic resistance might be a common property of periplasmic binding proteins in *E. coli*.

Many of the surviving proteins have biological functions associated with the stationary phase (Table 2), in which *E. coli* needs to survive starvation and oxidative stress. Dps has a role in protecting DNA against oxidative stress during starvation,<sup>29</sup> and its gene is one of the genes induced most strongly by hydrogen peroxide.<sup>30</sup> Iron and manganese superoxide dismutases are also important in protecting *E. coli* against oxidative stress during starvation.<sup>31</sup> Bacterioferritin, a Dps homolog, also sequesters excess iron in a non-toxic form in the central cavity inside the spherical 24-mer.<sup>32</sup> These

biochemical functions strongly suggest that their proteolytic resistance is related to their role in stress response.

Since cytosolic proteins are not likely to be exposed to exogenous proteases, the biological benefit of proteolytic resistance for the cytosolic survivors is less obvious. It might increase the lifetime of these proteins by protecting them from endogenous protease activities;<sup>33</sup> or, it might be an indication of conformational rigidity evolved to minimize any unwanted modification, such as deamidation.<sup>34</sup> Increasing the lifetime of proteins essential for stationary phase would thereby decrease the need for protein synthesis, which is an expensive process for *E. coli* in the stationary phase.

### *In vivo* degradation of proteolytically resistant proteins

How are these proteolytically resistant proteins degraded *in vivo*? Proteins induced specifically in stationary phase, such as Dps, need to be degraded rapidly when *E. coli* re-enters growth phase. Recently, Dps was found to have a degradation sequence at its N terminus for an ATP-dependent protease, ClpXP.<sup>35</sup> Interestingly, N-terminal sequencing of Dps from the 2-D gel showed that trypsin cleaved this degradation sequence (data not shown). These N-terminal residues are also not ordered in the Dps structure solved by X-ray crystallography.<sup>36</sup> Therefore, Dps has a highly flexible N-terminus, which is cleaved readily by trypsin or recognized by ClpXP. The rest of the protein is, however, resistant to proteolysis, which would ensure *in vivo* stability of the protein in the absence of proteolysis by ClpXP. This rigid structure tagged with a degradation signal within a flexible terminus seems to be an effective strategy to control the degradation of a protein exclusively by ATP-dependent proteases.

### Thermodynamic and kinetic requirements for survival

What does it mean to be a survivor? When the overall proteolysis rate constant is  $k_p$ , the fraction of survival as a function of time ( $f_s$ ) is:

$$f_s = \frac{N}{N_0} = e^{-k_p t}, \quad (4)$$

where  $N_0$  and  $N$  are the concentrations of intact proteins at  $t=0$  and after incubating for time  $t$ , respectively. Using the protease concentration (12  $\mu\text{M}$ ) and  $k_{\text{cat}}/K_M$  for the cleavage of ABZ-Ala-Gly-Leu-Ala-pNA, a generic thermolysin substrate ( $7.3 \times 10^5 \text{ M}^{-1}\text{s}^{-1}$ ),<sup>19</sup> the  $k_{\text{int}}$  value under the conditions of the survival assay with thermolysin is estimated to be  $8.8 \text{ s}^{-1}$ . With this estimated  $k_{\text{int}}$  value,  $k_p$  can be calculated for any given  $k_{\text{op}}$  and  $k_{\text{cl}}$  using equation (1). Also, the fraction of survival ( $f_s$ ) can be calculated for given  $k_{\text{op}}$  and  $k_{\text{cl}}$  with equation (4). Figure 7 shows the color-coded contour diagram



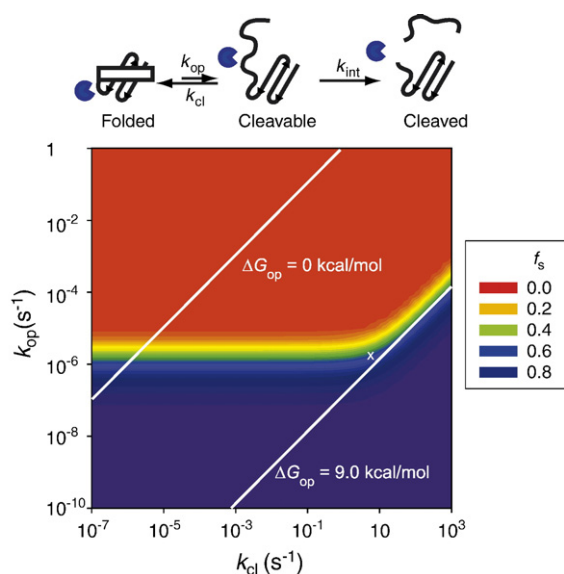


**Figure 7.** Contour diagram of the fraction of survival. The fraction of survival ( $f_s$ ) at the end of the assay with thermolysin is determined with equations (1) and (4) using  $k_{int}$  of  $8.8 \text{ s}^{-1}$ .  $k_{op}$  and  $k_{cl}$  are the forward and reverse rate constants for opening to the cleavable state.  $k_{int}$  is the intrinsic rate constant for proteolysis of proteins in the cleavable state. The  $k_{op}$  and  $k_{cl}$  values giving  $\Delta G_{op}$  of 0 kcal/mol and 9.0 kcal/mol are indicated with white continuous lines. Cleavable states in the red region are accessible under the assay condition and proteins with a cleavable state in the red region cannot pass the survival assay. The white  $\times$  symbol indicates the location of the cleavable state of MBP through which this protein is digested by thermolysin.

of the fraction of survival at each  $k_{op}$  and  $k_{cl}$ . The diagram shows a clear transition zone between a phase of survival (purple) and complete digestion (red).

The transition zone shows a kink in the region where  $k_{cl} \sim k_{int}$  ( $8.8 \text{ s}^{-1}$ ). When  $k_{cl} \ll k_{int}$ , the survival is independent of  $k_{cl}$ , which is equivalent to the EX1 regime in hydrogen exchange.<sup>8</sup> In this kinetic regime, overall proteolysis is determined only by  $k_{op}$ . Under the given assay condition 50% of a protein remains intact if the protein has  $k_{op} \sim 2 \times 10^{-6} \text{ s}^{-1}$  ( $t_{1/2} \sim$ four days) regardless of  $k_{cl}$ . When  $k_{cl} \gg k_{int}$ , the transition zone in Figure 7 shows another kinetic regime where the fraction of survival depends on both of  $k_{op}$  and  $k_{cl}$ , which is equivalent to the EX2 regime in hydrogen exchange.<sup>8</sup> Therefore, in this kinetic regime the survival depends on the free energy, and not the rate, of the opening step ( $\Delta G_{op}$ ). Under the given assay condition 50% of a protein remains intact if the  $\Delta G_{op}$  for the lowest cleavable state is 9.0 kcal/mol. The  $k_{op}$  and  $k_{cl}$  giving  $\Delta G_{op}$  values of 9.0 kcal/mol are indicated with a white line in Figure 7. Cleavable states lying below this line are not accessible thermodynamically under the given assay condition. Also, the  $k_{op}$  and  $k_{cl}$  giving  $\Delta G_{op}$  values of 0 kcal/mol is indicated in Figure 7. This line shows a region where kinetic stability (extremely small  $k_{op}$ ) can protect a protein in spite of

thermodynamic instability (a triangular purple region above the white line of  $\Delta G_{op} = 0 \text{ kcal/mol}$ ). Indeed this region has already been proven by the example of  $\alpha$ -lytic protease.<sup>16</sup>

Globally unfolded states of a protein are also cleavable states. To be a survivor, the globally unfolded states should not be accessible kinetically or thermodynamically under the assay condition. In other words, it is a necessity that the globally unfolded states of survivors should be within the purple region in Figure 7.

### Kinetic barrier protecting maltose binding protein from proteolysis by thermolysin

The location in Figure 7 of a cleavable state can be determined experimentally by measuring the rate of proteolysis,  $k_p$ . The  $k_{op}$  and  $K_{op}$  values for the cleavable state of MBP by thermolysin were determined to be  $1.8 \times 10^{-6} \text{ s}^{-1}$  and  $4.9 \times 10^{-7}$  from  $k_p$  measured at different protease concentrations (Figure 5(a)). From these values,  $k_{cl}$  is also calculated as  $3.6 \text{ s}^{-1}$ . The cleavable state of this protein is at the edge of the survival zone in Figure 7 (marked with a white X). The  $k_{cl}$  value ( $3.6 \text{ s}^{-1}$ ) is close to, but still smaller than,  $k_{int}$  ( $8.8 \text{ s}^{-1}$ ), which locates the proteolysis kinetics of this protein is at the boundary of the EX1 regime. The energy of the cleavable state ( $8.6 \text{ kcal/mol}$ ) is smaller than  $\Delta G_{op}$  for 50% survival of proteins in EX2 regime ( $9.0 \text{ kcal/mol}$ ). Therefore, the energy of the cleavable state would not be high enough to protect the protein, if proteolysis of MBP by thermolysin were in the EX2 regime.

The energy diagram of MBP proteolysis by thermolysin is depicted in Figure 8 using the determined kinetic constants. The energy of the cleavable state is much lower than the global stability of MBP ( $14.6(\pm 0.7) \text{ kcal/mol}$ ). However,  $k_{op}$  ( $1.8 \times 10^{-6} \text{ s}^{-1}$ ) is quite close to the global unfolding rate constant for MBP determined by urea denaturation ( $1.3 \times 10^{-6} \text{ s}^{-1}$ ), which suggests that the kinetic barrier to the cleavable state is the same kinetic barrier determining the global unfolding rate. It is also likely that this cleavable state is one of the kinetic intermediates on the unfolding pathway. This kinetic intermediate does not accumulate during unfolding, because the state exists after the rate-determining step. Considering the reversibility of protein folding, this intermediate could be on the folding trajectory of MBP.

This analysis of proteolysis kinetics suggests how MBP achieves proteolytic resistance to thermolysin. First, local fluctuations under native states are minimal. MBP does not expose cleavable sequences for thermolysin digestion without crossing the major kinetic barrier for global unfolding. Next, this kinetic barrier is considerably high. This slow unfolding controls overall proteolysis rate when the protein is surrounded with high concentration of proteases. This strategy used by MBP for proteolytic resistance against proteolysis is well consistent with the case in  $\alpha$ -lytic protease that employs the same strategy to the more extreme degree.<sup>16</sup> Kinetic

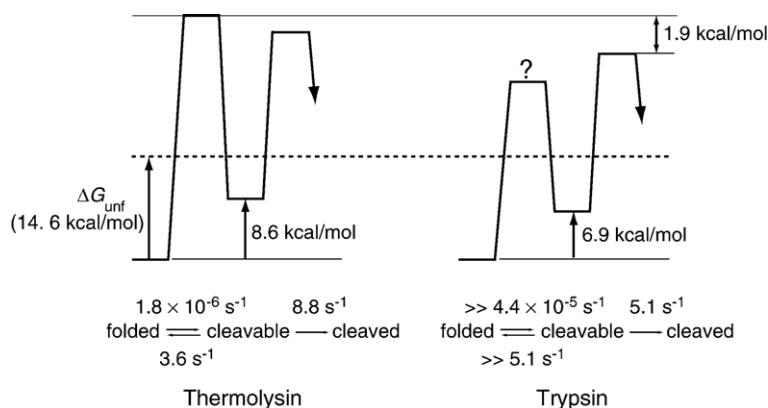


**Figure 8.** Reaction energy diagrams of MBP proteolysis by thermolysin and trypsin. The energy diagrams were depicted based on the kinetic data from proteolysis of MBP and the  $k_{cat}/K_M$  values determined with peptide substrates. The energy of globally unfolded state of MBP (14.6 kcal/mol) is indicated by a broken line. The access to the cleavable state is rate-determining in proteolysis of MBP by thermolysin, while the intrinsic proteolysis step is rate-determining in proteo-

lysis by trypsin. A question mark indicates that the absolute height of the energy barrier is not known from the available data.

stability has been proposed as a result of the evolution, creating the protective role of a high unfolding barrier.<sup>37–39</sup> The slow unfolding and proteolytic resistance of MBP supports this protective role of kinetic stability.

The proteolysis of MBP by trypsin is distinct from that with thermolysin digestion (Figure 5(b)). Even at 0.40 mg/ml trypsin, the kinetic constant does not show any sign of saturation. Therefore, only  $K_{op}$  could be determined ( $8.3 \times 10^{-6}$ ). The energy diagram of proteolysis of MBP by trypsin is also depicted in Figure 8. The  $k_{int}$  value was calculated to be  $5.1 \text{ s}^{-1}$  with the concentration of trypsin (0.40 mg/ml;  $17 \mu\text{M}$ ) and the  $k_{cat}/K_M$  values measured with insulin  $\beta$ -chain for trypsin ( $3.0 \times 10^5 \text{ M}^{-1}\text{s}^{-1}$ ).<sup>20</sup> From the comparison of proteolysis kinetics of MBP by trypsin and thermolysin, it is clear that the cleavable states for the two proteases are distinct and the cleavable state for trypsin digestion is apparently not susceptible to thermolysin. The cleavable state for trypsin digestion is lower by 1.7 kcal/mol than the cleavable state for thermolysin digestion (6.9 kcal/mol *versus* 8.6 kcal/mol). The kinetic barrier to the cleavable state is also much lower for trypsin digestion, which does not show the saturation behavior; the intrinsic proteolysis step is still rate-limiting even with 0.40 mg/ml of trypsin. Therefore, the  $k_{op}$  value, which cannot be determined with the data in Figure 5(b), is much greater than the proteolysis rate with 0.40 mg/ml trypsin ( $4.4 \times 10^{-5} \text{ s}^{-1}$ ) and  $k_{cl}$  is much greater than  $k_{int}$  ( $5.1 \text{ s}^{-1}$ ). Overall, proteolysis of MBP by 0.40 mg/ml trypsin ( $4.4 \times 10^{-5} \text{ s}^{-1}$ ) is faster than the opening to the cleavable state for thermolysin digestion ( $1.8 \times 10^{-6} \text{ s}^{-1}$ ); the rate-limiting step of trypsin digestion is lower by 1.9 kcal/mol than that of thermolysin digestion. The cleavable state for trypsin digestion seems to be accessible by local fluctuation: localized unfolding without global conformational change. Proteolysis through local fluctuation is consistent with the observations that this conformation does not expose any sequences cleavable by thermolysin and the transition from the cleavable to the folded conformation seems quite fast, compared with the intrinsic proteolysis (Figure 8).

## Energetics-based protein profiling

Proteomic studies have characteristically focused on the functions, interactions, and regulation of proteins on a genome-wide scale. We have developed a novel approach of applying proteomic methods to studying energetic properties of proteins. In the studies reported here, we used proteolysis as a structural probe to identify proteins with energy landscapes resistant to proteolysis. The identified rigid proteins may have biotechnological applications. For instance, proteolytic resistance in proteins can ensure a longer lifetime in harsh environments. The proteins identified through this survival assay may be suitable for such engineering applications as is, or as templates for protein engineering. Modification of this method should enable us to analyze proteomes according to other interesting energetic properties, such as thermal stability, kinetic stability, and resistance to chemical denaturants. Energetics-based protein profiling on a proteomic scale will allow us to understand better how conformational energy landscapes are encoded by sequences and structures, and how these energetic properties are related to biological functions. This understanding also will provide important basic knowledge for designing functional proteins with proper dynamics and energetics for their biochemical functions.

## Materials and Methods

### Preparation of soluble fraction of *E. coli*

*E. coli* K12 was grown overnight in 50 ml of Luria Bertani (LB) medium and harvested. The cell pellet was resuspended in 50 ml of 20 mM Tris-HCl (pH 8.0), containing 10 mM EDTA (pH 8.0) and 250 mM NaCl, then pelleted again by centrifugation. The washed cell pellet was resuspended in 10 ml of 20 mM Tris-HCl (pH 8.0), containing 1 mM EDTA (pH 8.0) and 50 mM NaCl. The cells were lysed by lysozyme treatment and sonication, and centrifuged to remove cell debris and the membrane fraction. To prevent nucleic acids from protecting proteins against proteolysis by forming complexes, the resulting supernatant was incubated with 0.1 mg/ml DNase I and

0.1 mg/ml RNase A. MgCl<sub>2</sub> and CaCl<sub>2</sub> were added to 2.5 mM and 1.0 mM, respectively, for this digestion reaction. To minimize the interference from small metabolites and digested nucleic acids, the lysate was dialyzed first against 20 mM Tris-HCl (pH 8.0) containing 250 mM NaCl and then against 20 mM Tris-HCl (pH 8.0). The lysate was sterilized by passing through a 0.20 µm syringe filter and stored at -20 °C until used.

### Proteolysis of *E. coli* proteome

Proteolysis of *E. coli* lysate was performed in 20 mM Tris-HCl (pH 8.0) containing 10 mM CaCl<sub>2</sub> and 50 mM NaCl. The reaction was initiated by adding trypsin (Sigma, St. Louis, MO) or thermolysin (Sigma, St. Louis, MO) to the final concentration of 0.40 mg/ml and incubated at 25 °C for four days. Samples were taken at a designated time points to monitor the progress of proteolytic digestion by SDS-PAGE. The activity of trypsin in the proteolysis reaction was determined by monitoring the cleavage of N<sub>α</sub>-*p*-tosyl-L-arginine methyl ester (TAME) (Sigma, St. Louis, MO) spectrophotometrically at 247 nm. The activity of thermolysin in the reaction was determined by monitoring the cleavage of *o*-aminobenzoyl-Ala-Gly-Leu-Ala-*p*-nitrobenzylamide (ABZ-Ala-Gly-Leu-Ala-*p*NA; MD Biosciences, St. Paul, MN) with a fluorometer.

### 2-D electrophoresis and protein identification

To identify the survivors, *E. coli* lysate was incubated with 0.40 mg/ml trypsin or 0.40 mg/ml thermolysin in 20 mM Tris-HCl (pH 8.0) containing 10 mM CaCl<sub>2</sub> and 50 mM NaCl at 25 °C for four days. 10 µl of 0.50 M EDTA (pH 8.0) (for thermolysin) or 0.10 M phenylmethylsulfonyl fluoride (for trypsin) was added to 240 µl of reactions to quench further proteolysis. 2-D gel electrophoresis was performed as described by the manufacturer.<sup>40</sup> Proteins in samples were precipitated by acetone. Pellets were dissolved in the rehydration buffer (8 M urea, 20 mM DTT, 2% Chaps, 2.0% IPG buffer, 0.002% bromophenol blue). The proteins in the rehydration buffer were separated with 13 cm Immobiline Drystrips, pH 3–10 NL (Amersham, Piscataway, NJ) in the first dimension and with continuous 15% (w/v) SDS gels in the second dimension. Gels were stained by Colloidal Blue staining reagent (Invitrogen, Carlsbad, CA). Spots on the gels were cut and digested with Montage In-Gel Digest<sub>zP</sub> Kit (Millipore, Billerica, MA). About 1 µl of the tryptic peptide mixture from each gel spot was combined with an equal volume of matrix solution and allowed to dry on a MALDI target. The matrix solution used was a 10 mg/ml solution of alpha-cyano-4-hydroxycinnamic acid in 0.1% TFA/50% acetonitrile. Mass spectra were acquired on a Bruker (Billerica, MA) Reflex III mass spectrometer. Proteins corresponding to each spot were identified by a web-based software, MS-FIT†.

### Determination of proteolysis kinetics of maltose binding protein

The coding region for maltose binding protein (*malE*) was amplified by polymerase chain reaction, cloned, and expressed under the control of the T7 promoter. Maltose

binding protein was purified with ion-exchange and gel filtration chromatography. The purity of each protein was verified using SDS-PAGE and mass spectroscopy.

Proteolysis kinetics was determined based on the method reported elsewhere.<sup>8</sup> 0.50 mg/ml maltose binding protein was incubated at 25 °C with 0.40 mg/ml thermolysin or 0.40 mg/ml trypsin in 20 mM Tris-HCl buffer (pH 8.0), containing 50 mM NaCl and 10 mM CaCl<sub>2</sub>. For thermolysin digestion, 15 µl of the reaction was removed at each time point and quenched by adding 5 µl of 50 mM EDTA (pH 8.0). For trypsin digestion, 18 µl of the reaction was removed and quenched by adding 2 µl of 0.1 M PMSF in ethanol. 20 µl of SDS sample buffer was then added to each quenched reaction and boiled. 10 µl of the mixture was used for SDS-PAGE. Gels were stained with Sypro Red fluorescent dye (Molecular Probes, Eugene, OR) and scanned with Typhoon imaging system (GE Healthcare, Piscataway, NJ). Proteolysis kinetic constants (*k<sub>p</sub>*) were determined by monitoring the change in intensity of intact protein bands. Determined kinetic constants were fit to equation (2) to determine *k<sub>op</sub>* and *K<sub>op</sub>*.

### Acknowledgements

We thank Kael F. Fischer for discussions and suggestions in development of the project; James A. Blair and Arnab Chowdry for their technical assistance; Alan Sachs, Eric N Nicholson, Srebrenka Robic, Erik J. Miller, Elizabeth A. Shank, David E. Wildes, Jason F. Cellitti, and Tracy A. Young for thoughtful comments on the manuscript. This work was supported by Grant GM50945 (NIH).

### References

1. Frauenfelder, H., Sligar, S. G. & Wolynes, P. G. (1991). The energy landscapes and motions of proteins. *Science*, **254**, 1598–1603.
2. Bai, Y., Sosnick, T. R., Mayne, L. & Englander, S. W. (1995). Protein folding intermediates: native-state hydrogen exchange. *Science*, **269**, 192–197.
3. Chamberlain, A. K., Handel, T. M. & Marqusee, S. (1996). Detection of rare partially folded molecules in equilibrium with the native conformation of RNase H. *Nature Struct. Biol.* **3**, 782–787.
4. Kern, D., Volkman, B. F., Luginbuhl, P., Nohaile, M. J., Kustu, S. & Wemmer, D. E. (1999). Structure of a transiently phosphorylated switch in bacterial signal transduction. *Nature*, **402**, 894–898.
5. Eisenmesser, E. Z., Bosco, D. A., Akke, M. & Kern, D. (2002). Enzyme dynamics during catalysis. *Science*, **295**, 1520–1523.
6. Parsell, D. A. & Sauer, R. T. (1989). The structural stability of a protein is an important determinant of its proteolytic susceptibility in *Escherichia coli*. *J. Biol. Chem.* **264**, 7590–7595.
7. Matouschek, A. (2003). Protein unfolding - an important process *in vivo*? *Curr. Opin. Struct. Biol.* **13**, 98–109.
8. Park, C. & Marqusee, S. (2004). Probing the high energy states in proteins by proteolysis. *J. Mol. Biol.* **343**, 1467–1476.
9. Imoto, T., Yamada, H. & Ueda, T. (1986). Unfolding rates of globular proteins determined by kinetics of proteolysis. *J. Mol. Biol.* **190**, 647–649.

† <http://www.prospector.ucsf.edu/ucsfhtml4.0/msfit.htm>

10. Fontana, A., Polverino de Lauro, P., De Filippis, V., Scaramella, E. & Zamboni, M. (1997). Probing the partly folded states of proteins by limited proteolysis. *Fold. Des.* **2**, R17–R26.
11. Tyndall, J. D., Nall, T. & Fairlie, D. P. (2005). Proteases universally recognize beta strands in their active sites. *Chem. Rev.* **105**, 973–999.
12. Linderström-Lang, K. (1938). Peptide bonds in globular proteins. *Nature*, **142**, 996.
13. Linderström-Lang, K. (1950). Structure and enzymatic break-down of proteins. *Cold Spring Harbor Symp. Quant. Biol.* **14**, 117–126.
14. Anfinsen, C. B. & Scheraga, H. A. (1975). Experimental and theoretical aspects of protein folding. *Advan. Protein Chem.* **29**, 205–300.
15. Wang, L. & Kallenbach, N. R. (1998). Proteolysis as a measure of the free energy difference between cytochrome c and its derivatives. *Protein Sci.* **7**, 2460–2664.
16. Jaswal, S. S., Sohl, J. L., Davis, J. H. & Agard, D. A. (2002). Energetic landscape of  $\alpha$ -lytic protease optimizes longevity through kinetic stability. *Nature*, **415**, 343–346.
17. Keil, B. (1992). *Specificity of Proteolysis*. Springer-Verlag, New York.
18. Cunningham, E. L., Jaswal, S. S., Sohl, J. L. & Agard, D. A. (1999). Kinetic stability as a mechanism for protease longevity. *Proc. Natl Acad. Sci. USA*, **96**, 11008–11014.
19. Park, C. & Marqusee, S. (2005). Pulse proteolysis: a simple method for quantitative determination of protein stability and ligand binding. *Nature Methods*, **2**, 207–212.
20. Corey, D. & Craik, C. (1992). An investigation into the minimum requirements for peptide hydrolysis by mutation of the catalytic triad of trypsin. *J. Am. Chem. Soc.* **114**, 1784–1790.
21. Hollien, J. & Marqusee, S. (1999). A thermodynamic comparison of mesophilic and thermophilic ribonucleases H. *Biochemistry*, **38**, 3831–3836.
22. Szilágyi, A. & Závodszy, P. (2000). Structural differences between mesophilic, moderately thermophilic and extremely thermophilic protein subunits: results of a comprehensive survey. *Struct. Fold. Des.* **8**, 493–504.
23. Sun, Y. J., Rose, J., Wang, B. C. & Hsiao, C. D. (1998). The structure of glutamine-binding protein complexed with glutamine at 1.94 Å resolution: comparisons with other amino acid binding proteins. *J. Mol. Biol.* **278**, 219–229.
24. Quioco, F. A., Spurlino, J. C. & Rodseth, L. E. (1997). Extensive features of tight oligosaccharide binding revealed in high-resolution structures of the maltodextrin transport/chemosensory receptor. *Structure*, **5**, 997–1015.
25. Awaeva, S., Kurilova, S., Nazarova, T., Rodina, E., Vorobyeva, N., Sklyankina, V. *et al.* (1997). Crystal structure of *Escherichia coli* inorganic pyrophosphatase complexed with  $\text{SO}_4^{2-}$ . Ligand-induced molecular asymmetry. *FEBS Letters*, **410**, 502–508.
26. Koellner, G., Luic, M., Shugar, D., Saenger, W. & Bzowska, A. (1998). Crystal structure of the ternary complex of *E. coli* purine nucleoside phosphorylase with formycin B, a structural analogue of the substrate inosine, and phosphate (sulphate) at 2.1 Å resolution. *J. Mol. Biol.* **280**, 153–166.
27. Duée, E., Olivier-Deyris, L., Fanchon, E., Corbier, C., Branlant, G. & Dideberg, O. (1996). Comparison of the structures of wild-type and a N313T mutant of *Escherichia coli* glyceraldehyde 3-phosphate dehydrogenase: implication for NAD binding and cooperativity. *J. Mol. Biol.* **257**, 814–838.
28. Oliver, D. B. (1996). Periplasm. In *Escherichia coli and Salmonella: Cellular and Molecular Biology* 2nd edit. (Neidhardt, F. C., ed.), vol. 1, pp. 88–103. 2 vols. ASM Press, Washington, DC.
29. Martinez, A. & Kolter, R. (1997). Protection of DNA during oxidative stress by the nonspecific DNA-binding protein Dps. *J. Bacteriol.* **179**, 5188–5194.
30. Zheng, M., Wang, X., Templeton, L. J., Smulski, D. R., LaRossa, R. A. & Storz, G. (2001). DNA microarray-mediated transcriptional profiling of the *Escherichia coli* response to hydrogen peroxide. *J. Bacteriol.* **183**, 4562–4570.
31. Dukan, S. & Nystrom, T. (1999). Oxidative stress defense and deterioration of growth-arrested *Escherichia coli* cells. *J. Biol. Chem.* **274**, 26027–26032.
32. Andrews, S. C., Le Brun, N. E., Barynin, V., Thomson, A. J., Moore, G. R., Guest, J. R. & Harrison, P. M. (1995). Site-directed replacement of the coaxial heme ligands of bacterioferritin generates heme-free variants. *J. Biol. Chem.* **270**, 23268–23274.
33. Gottesman, S. (1996). Proteases and their targets in *Escherichia coli*. *Annu. Rev. Genet.* **30**, 465–506.
34. Robinson, N. E. & Robinson, A. B. (2001). Molecular clocks. *Proc. Natl Acad. Sci. USA*, **98**, 944–949.
35. Flynn, J. M., Neher, S. B., Kim, Y. I., Sauer, R. T. & Baker, T. A. (2003). Proteomic discovery of cellular substrates of the ClpXP protease reveals five classes of ClpX-recognition signals. *Mol. Cell*, **11**, 671–683.
36. Grant, R. A., Filman, D. J., Finkel, S. E., Kolter, R. & Hogle, J. M. (1998). The crystal structure of Dps, a ferritin homolog that binds and protects DNA. *Nature Struct. Biol.* **5**, 294–303.
37. Plaza del Pino, I. M., Ibarra-Molero, B. & Sanchez-Ruiz, J. M. (2000). Lower kinetic limit to protein thermal stability: a proposal regarding protein stability *in vivo* and its relation with misfolding diseases. *Proteins: Struct. Funct. Genet.* **40**, 58–70.
38. Scalley-Kim, M. & Baker, D. (2004). Characterization of the folding energy landscapes of computer generated proteins suggests high folding free energy barriers and cooperativity may be consequences of natural selection. *J. Mol. Biol.* **338**, 573–583.
39. Godoy-Ruiz, R., Ariza, F., Rodriguez-Larrea, D., Perez-Jimenez, R., Ibarra-Molero, B. & Sanchez-Ruiz, J. M. (2006). Natural selection for kinetic stability is a likely origin of correlations between mutational effects on protein energetics and frequencies of amino acid occurrences in sequence alignments. *J. Mol. Biol.* **362**, 966–978.
40. Berkelman, T. & Stenstedt, T. (1998). *2-D Electrophoresis Using Immobilized pH Gradients: Principles and Methods*, Amersham Bioscience, Piscataway, NJ.
41. Kraulis, P. J. (1991). MOLSCRIPT: A program to produce both detailed and schematic plots of protein structures. *J. Appl. Crystallog.* **24**, 946–950.

Edited by C. R. Matthews

(Received 2 November 2006; received in revised form 15 February 2007; accepted 22 February 2007)  
Available online 7 March 2007